

# A Novel Approach for Estimating Positive Lyapunov Exponents in One-Dimensional Chaotic Time Series Using Machine Learning

Velichko A. \*, Belyaev M., Boriskov P.

Institute of Physics and Technology, Petrozavodsk State University, 185910 Petrozavodsk, Russia

\*Email: velichkogf@gmail.com

## Abstract

Understanding and quantifying chaos in nonlinear dynamical systems remains a fundamental challenge in science and engineering. The Lyapunov exponent is a key measure of chaotic behavior, but its accurate estimation from experimental data is often hindered by methodological and computational limitations. In this work, we present a novel machine-learning-based approach for estimating the positive Lyapunov exponent (MLE) from one-dimensional time series, using the growth of out-of-sample prediction errors as a proxy for trajectory divergence.

Our method demonstrates high scientific relevance, offering a robust, data-driven alternative to traditional analytic techniques. Through comprehensive testing on several canonical chaotic maps — including the logistic, sine, cubic, and Chebyshev maps — we achieved a coefficient of determination  $R^2_{\text{pos}} > 0.9$  between predicted and theoretical MLE values for time series as short as  $M = 200$  points. The best accuracy was observed for the Chebyshev map ( $R^2_{\text{pos}} = 0.999$ ). Notably, the proposed method maintains high computational efficiency and generalizes well across various machine learning algorithms.

These results highlight the significance of our approach for practical chaos analysis in both synthetic and experimental settings, opening new possibilities for robust nonlinear dynamics assessment when only time series data are available.

## I. Introduction

Chaos theory explores the behavior of nonlinear dynamical systems that, despite being deterministic, exhibit unpredictably complex patterns sensitive to initial conditions. Such sensitivity, popularly known as the "butterfly effect" <sup>1,2</sup> underscores that small variations in the starting state of a system can lead to significantly divergent outcomes over time. One of the key quantitative measures for characterizing this sensitivity and the chaotic nature of these systems is the Lyapunov exponent <sup>3–5</sup>.

Lyapunov exponents measure the exponential rate of divergence or convergence of initially close trajectories in a dynamical system, thereby quantifying the degree of instability within the system. A positive Lyapunov exponent indicates chaos, signifying that trajectories diverge exponentially, resulting in unpredictable long-term behavior. Conversely, negative exponents denote convergence and stability, while zero exponents typically correspond to neutral, periodic, or quasiperiodic behavior <sup>1,2</sup>.

The accurate calculation and interpretation of Lyapunov exponents is essential, as these values are directly connected to system predictability and stability. Specifically, they allow researchers and practitioners to evaluate how quickly small errors or uncertainties grow, providing critical insights into the reliability of predictions made by models describing complex systems.

Systems characterized by predominantly positive Lyapunov exponents, such as those encountered in meteorology or ecological modeling, present significant challenges due to their reduced predictability and inherent sensitivity to small disturbances <sup>6–8</sup>.

Accurate estimation of Lyapunov exponents drives progress in diverse fields. In meteorology and ecology, they enable real-time adaptive corrections that sharpen forecasts and optimize resource use <sup>6</sup>. In mechanical and aerospace engineering—e.g., helicopter flight dynamics—they expose incipient instabilities, helping engineers design safer control strategies <sup>6</sup>. Electrical-power operators rely on them to trace transient-stability margins and make rapid security assessments after disturbances <sup>7,11</sup>. Underlying these successes is the positive Lyapunov exponent, which quantifies the exponential divergence of nearby trajectories and thereby captures a system's sensitivity to initial conditions—the hallmark of chaos <sup>12,13</sup>.

Quantitatively, the magnitude of the positive Lyapunov exponent directly correlates with the rate at which prediction errors or uncertainties in initial states amplify over time. Hence, knowledge of this value is critical for predicting the reliability of long-term forecasts and understanding the limits of predictability inherent in the system under study <sup>14–16</sup>.

From a practical and methodological perspective, calculating the positive Lyapunov exponent is crucial for the development and validation of computational algorithms used in chaos analysis. Advanced methods, including traditional numerical techniques and modern machine learning algorithms, have been specifically designed and refined to efficiently and accurately estimate this exponent, underscoring its central role in the practical analysis of complex dynamical systems <sup>17,18</sup>.

Traditionally, these exponents have been calculated using various approaches, such as local trajectory integration <sup>19</sup>, nonparametric regression <sup>20</sup>, pseudo-orbits <sup>21</sup>, eigenvalue decomposition <sup>22</sup>, time series analysis <sup>12,23</sup>, and symplectic methods for Hamiltonian systems <sup>24</sup>. Each method has distinct advantages, such as accuracy, robustness to data changes, or reduced computational complexity.

In the context of machine learning approaches for estimating Lyapunov exponents, two primary directions can be distinguished. In the first case, the exponent values are directly approximated by a trained model from input time series data <sup>6,20,25,26</sup>. Supervised learning methods—including regression trees <sup>6</sup>, multilayer perceptrons, convolutional neural networks (CNNs), and long short-term memory (LSTM) networks — have demonstrated accurate predictions of stable exponents, reasonable approximations for unstable exponents, and modest success with neutral exponents, especially in locally homogeneous attractors. Reservoir computing, leveraging a high-dimensional dynamical system to replicate chaotic attractors, has proven effective for complex dynamics such as those in the Lorenz and Kuramoto-Sivashinsky systems <sup>27</sup>. CNN-based deep learning has successfully handled hyperchaotic scenarios <sup>26</sup>.

In the second case, the exponents are estimated indirectly, based on the analysis of the divergence between two nearby trajectories <sup>17,21,23</sup>. The latter approach is typically utilized to estimate only the largest Lyapunov exponent, which, however, is the most critical indicator for characterizing the chaotic behavior of nonlinear systems.

In addition to the above-mentioned methods, another indirect but insightful approach involves estimating the Lyapunov exponent through the entropy of a time series, as these parameters are inherently interconnected. Typically, higher entropy corresponds to a higher Lyapunov exponent, reflecting increased dynamical instability and unpredictability. However, this relationship provides only an approximate estimation and should be interpreted with caution. Recent studies

by our group have extended these concepts by introducing modern entropy metrics, such as Neural Network Entropy (NNetEn)<sup>28</sup> and Logistic Neural Network (LogNNet)<sup>29</sup>, specifically designed to quantify complexity within neural network contexts. Both NNetEn and LogNNet quantify complexity through nonlinear transformations of input data using chaotic or reservoir computing principles, and thus are closely related to Lyapunov exponents and traditional entropy measures. In practical contexts such as nonequilibrium statistical mechanics and transport phenomena, the difference between positive Lyapunov exponents and Kolmogorov–Sinai entropy per unit time is critical to understanding fractal dynamics and chaotic transport processes<sup>30</sup>.

Machine learning methods notably reduce computational cost compared to traditional methods, which often involve intricate mathematical operations and large-scale data handling. Nevertheless, their accuracy is influenced by the system's characteristics and attractor homogeneity. Collectively, these ML techniques offer a promising, computationally efficient approach to enhance the understanding and prediction capabilities for chaotic dynamical systems, complementing existing classical methodologies. These methods offer substantial improvements in computational efficiency, and potentially enhanced accuracy and robustness, providing a non-intrusive means of analyzing chaotic systems without directly relying on intensive mathematical computations<sup>3,6</sup>.

In this study, we attempt to combine both approaches by using machine learning methods to calculate the averaged divergence through prediction errors between sets of trajectories from test and training datasets. Unlike most previously cited works, the robustness of the proposed method is validated across a wide range of parameters in discrete mappings, employing various machine learning algorithms.

## 2. Methodology

### 2.1 Generation of Chaotic Time Series

In this study, chaotic time series were generated using four discrete maps: logistic, sine, cubic, and Chebyshev maps. Depending on the control parameter  $r$ , these maps can produce both regular and chaotic behavior. The following recursive formulas define each discrete map along with the ranges of the control parameter  $r$ :

$$\begin{cases} x_{m+1} = r \cdot x_m (1 - x_m), & 3.5 \leq r \leq 4, \text{ Logistic map} \\ x_{m+1} = r \cdot \sin(\pi x_m), & 0.85 \leq r \leq 1, \text{ Sine map} \\ x_{m+1} = r \cdot x_m (1 - x_m^2), & 2.3 \leq r \leq 3, \text{ Cubic map} \\ x_{m+1} = \cos(r \cdot \arccos(x_m)), & 1 \leq r \leq 10, \text{ Chebyshev map} \end{cases} \quad (1)$$

Each interval of the control parameter  $r$  was divided into 500 equidistant points. For each of these points, a time series of 10,000 data points was generated, with the initial 1,000 points discarded to mitigate transient effects. Thus, for each chaotic map under consideration, we obtained 500 distinct time series corresponding to different values of the parameter  $r$ .

### 2.2 Standard Method for Calculation of Lyapunov Exponents for Discrete Maps

Lyapunov exponent  $\lambda$  characterizes the regularity of a dynamic system, indicating how two trajectories in phase space, initially separated by distance  $\delta_0$ , diverge or converge over time  $t$ :

$$|\delta(t)| = |\delta_0| \cdot \exp(\lambda \cdot t). \quad (2)$$

For the discrete maps described in section 2.1, there is only one Lyapunov exponent. Generally, a dynamic system can have multiple Lyapunov exponents equal to the dimensionality of the phase space. However, the exponent with the largest value, the maximum Lyapunov exponent (MLE), predominantly determines the system's predictability. Thus, only the MLE, denoted  $\lambda$ , will be considered hereafter.

An advantage of discrete maps is the straightforward estimation of MLE based on theoretical considerations. The Lyapunov exponent of discrete map is calculated using the known limit <sup>31</sup>. Considering the discrete nature of the time series, equation (2) implies the following calculation for  $\lambda$ :

$$\lambda = \lim_{m \rightarrow \infty} \left( \frac{1}{m} \sum_{i=0}^{m-1} \ln \left( \left| f'(x_i) \right| \right) \right), \quad (3)$$

Here  $f$ , represents the recursive relationship defining each map (see equation (1)). For each of the 500 control parameter values  $r$ , the Lyapunov exponent was calculated using equation (3). The resulting curves served as reference values for evaluating the accuracy of the proposed method and computing error metrics (see section 2.5).

### 2.3 Calculation of Maximum Lyapunov Exponent Using Machine Learning

Based on equation (2) and considering the discrete nature of the time series, trajectory divergence after steps can be expressed as:

$$\ln(|\delta(N)|) = \ln(|\delta_0|) + \lambda \cdot N. \quad (4)$$

Thus, to estimate  $\lambda$ , it is necessary to determine the slope angle of the linear approximation for the curve  $\ln(|\delta(N)|)$ .

In this study, the mean absolute error (MAE) of predictions made by machine learning algorithms is proposed as an estimator for the absolute divergence  $|\delta(N)|$ . This error reflects how rapidly trajectories diverge within a time series as the prediction horizon  $N$  increases.

To estimate the maximum Lyapunov exponent using machine learning methods ( $\lambda_{ml}$ ), the following procedure is implemented:

1. For each prediction horizon  $N = 1..K$ , the original time series  $X = \{x_1, x_2, \dots, x_M\}$  of length  $M$  is divided into segments of length  $L$  (where  $L < M$ ), creating the input feature set  $X_{ml}$  as follows:  $X_{ml} = \{\{x_1, x_2, \dots, x_L\}, \{x_2, x_3, \dots, x_{L+1}\}, \dots, \{x_{M-L-N-1}, x_{M-L-N}, \dots, x_{M-N}\}\}$ . Correspondingly, the target variable set  $Y_{ml}$  is formed by selecting the points located exactly  $N$  steps ahead of each segment:  $Y_{ml} = \{x_{L+N}, x_{L+N+1}, \dots, x_M\}$ . Thus, the input segments ( $X_{ml}$ ) represent the features, and the future values ( $Y_{ml}$ ) represent the target variable the algorithm aims to predict.
2. Both feature set  $X_{ml}$  and target variable set  $Y_{ml}$  are split into training and testing subsets, maintaining the same test subset proportion  $P$  for each prediction horizon  $N$ . The training subsets are used to train the machine learning algorithms, while the testing subsets are used to evaluate the MAE.
3. After training the MAE is calculated using testing subsets for each prediction horizon  $N$  as follows:

$$MAE = \sum_{i=1..s} \frac{|Y_{ml_i} - Y_i|}{s}, \quad (5)$$

where  $Y'$  is the set of predicted values generated by the machine learning model. Thus, we obtain the dependence of MAE on  $N$ .

4. Finally, a linear approximation is constructed using values of  $\ln[\text{MAE}(N)]$ , and the slope of this approximation ( $b$ ) provides the estimate of the maximum Lyapunov exponent ( $\lambda_{\text{ml}}$ ):

$$\lambda_{\text{ml}} = b = \frac{d(\ln[\text{MAE}(N)])}{dN}. \quad (6)$$

The rationale for interpreting MAE as trajectory divergence lies in the fact that machine learning models approximate training sets and predict test data based on this approximation. The prediction error represents the average deviation of test trajectories from the closest training trajectories.

Parameters of the proposed algorithm include the number of points  $K$ , segment length  $L$ , relative size of the test subset (to full dataset)  $P$ , and machine learning hyperparameters (see section 2.4). This method applies to stationary chaotic time series since the training-test split approach cannot adequately assess transient processes with changing amplitude values.

Specifically, the parameter  $K$  represents the number of prediction horizons  $N$  used in constructing the linear approximation (see Eq.6). The approximation starts from  $N = 1$ , and includes  $K$  consecutive values: for example, if  $K = 2$ , the linear fit is performed using  $N = 1, 2$ ; if  $K = 4$ , then  $N = 1, 2, 3, 4$ , and so on. It is evident that  $K > 1$  must hold, since a minimum of two points is required to construct a linear approximation.

The parameter  $L$  denotes the number of historical data points in each input segment used by the machine learning model for predicting future values.

## 2.4 Machine Learning Methods

To estimate  $\lambda_{\text{ml}}$  using MAE, several machine learning methods were selected, including both standard algorithms — such as k-nearest neighbors (KNN) <sup>32</sup>, random forest (RF), multilayer perceptron (MLP) <sup>33</sup> and a novel reservoir-based method employing KNN (R-KNN). The proposed R-KNN approach is described in detail in subsection 2.4.1.

Hyperparameters for KNN included the number of neighbors, weighting type, and distance function. For RF, hyperparameters included the number of trees, split quality evaluation criterion, maximum tree depth, minimum split size, and minimum leaf size. For MLP, hyperparameters comprised layer sizes and configurations, activation functions, learning rate, regularization strength, maximum training iterations, and minimum allowable deviation.

### 2.4.1 Reservoir-based Network with KNN (R-KNN)

Reservoir networks consist of interconnected neurons whose internal connection weights and input weights (used to pass features into reservoir neurons) are randomly initialized and remain unchanged during training. Only the weights connecting the reservoir neurons to the output linear layer are adjusted throughout training. This architecture represents a type of reservoir neural network known for high-accuracy predictions of chaotic time series<sup>34</sup>. Prominent examples of reservoir-based networks include echo state networks (ESN)<sup>35</sup>, LogNet<sup>36</sup>, and liquid state machines (LSM)<sup>34</sup>.

In this study, KNN was proposed as the output layer method, predicting time series values by comparing reservoir neuron activities. Given that the reservoir typically contains numerous neurons, principal component analysis (PCA)<sup>37</sup> is employed to reduce the dimensionality of the feature vector fed into KNN, significantly simplifying data representation with minimal loss of

information. Thus, reservoir neuron outputs undergo PCA transformation, after which KNN predicts the time series values.

The hyperparameters for the proposed method include reservoir properties (number of neurons, connectivity, spectral radius, activation function), input layer parameters (scaling factor, connectivity with reservoir neurons), PCA parameters (number of components), and the aforementioned KNN hyperparameters.

## 2.5 Method for Optimizing Parameters

To evaluate the accuracy of the calculated  $\lambda_{ml}$ , the deviation of  $\lambda_{ml}(r)$  from the reference values  $\lambda(r)$  obtained using the standard calculation method (section 2.2) was assessed. The coefficient of determination  $R^2$  was chosen as the metric for evaluating calculation errors, computed as follows. First, the average value  $\lambda'$  was calculated for all  $T = 500$  points in the range of the parameter  $r$ :

$$\lambda' = \frac{1}{T} \sum_{i=1}^T \lambda_i. \quad (7)$$

Next, the residual sum of squares  $SS_{res}$  and total sum of squares  $SS_{tot}$  were computed:

$$SS_{res} = \frac{1}{T} \sum_{i=1}^T (\lambda_i - \lambda_{ml_i})^2, \quad (8)$$

$$SS_{tot} = \sum_{i=1}^N (\lambda_i - \lambda')^2. \quad (9)$$

Using these sums, the coefficient of determination  $R^2$  was calculated:

$$R^2 = 1 - \frac{SS_{res}}{SS_{tot}}. \quad (10)$$

An  $R^2$  value closer to 1 indicates a stronger agreement between  $\lambda(r)$  and  $\lambda_{ml}(r)$ . It should be noted that the proposed method yields only positive values of  $\lambda_{ml}$ . Therefore, error evaluation was performed both for the entire curve ( $R^2_{tot}$ ) and exclusively for points where  $\lambda(r) \geq 0$  ( $R^2_{pos}$ ).

For each machine learning method and discrete map, parameters described in sections 2.3 and 2.4 were optimized to maximize  $R^2_{pos}$ , which is equivalent to maximizing  $R^2_{tot}$ .

## 3. Experimental Results

### 3.1 Analysis of the Proposed Method Efficiency

Table 1 presents the values of  $R^2_{pos}$  and  $R^2_{tot}$  for various machine learning methods and discrete maps. It should be emphasized that the presented results correspond to the optimal parameters that minimize the error.

Table 1. Error metrics ( $R^2_{pos}$  and  $R^2_{tot}$ ) for  $\lambda_{ml}(r)$  relative to reference  $\lambda(r)$  for various machine learning methods.

ML Algorithm	Logistic Map		Sine Map		Cubic Map		Chebyshev Map	
	$R^2_{pos}$	$R^2_{tot}$	$R^2_{pos}$	$R^2_{tot}$	$R^2_{pos}$	$R^2_{tot}$	$R^2_{pos}$	$R^2_{tot}$
KNN	0.923	0.781	0.895	0.826	0.948	0.895	0.999	0.999
RF	0.954	0.787	0.952	0.842	0.930	0.886	0.998	0.998
MLP	0.718	0.465	0.657	0.532	0.839	0.794	-0.662	-0.658
KNN-R	0.922	0.781	0.892	0.825	0.946	0.894	0.999	0.999

The metric  $R^2_{\text{pos}}$  for all maps exceeds 0.9, indicating a good degree of correspondence between  $\lambda_{\text{ml}}(r)$  and the reference curves  $\lambda(r)$ . The best match was observed for the Chebyshev map, achieving near-perfect results ( $R^2_{\text{pos}} = 0.999$ ). The highest accuracy was achieved by the KNN model for the cubic and Chebyshev maps and the RF model for logistic and sine maps. The performance of the KNN-R model closely mirrored that of the standard KNN. The MLP model exhibited the poorest performance, particularly for the Chebyshev map, and thus was excluded from subsequent analysis.

It is important to note that the  $R^2_{\text{tot}}$  metric is generally less meaningful because the proposed methodology cannot estimate negative Lyapunov exponents from slope angles. Additionally, during time series generation, initial transient values were discarded, resulting in constant or repeating values for segments corresponding to negative Lyapunov exponents. Therefore,  $R^2_{\text{tot}}$  is presented solely alongside  $R^2_{\text{pos}}$  for completeness.

Figure 1 shows the dependencies  $\lambda_{\text{ml}}(r)$  for the most accurate machine learning algorithms for each of the four maps (as identified in Table 1), alongside the reference curves  $\lambda(r)$ .

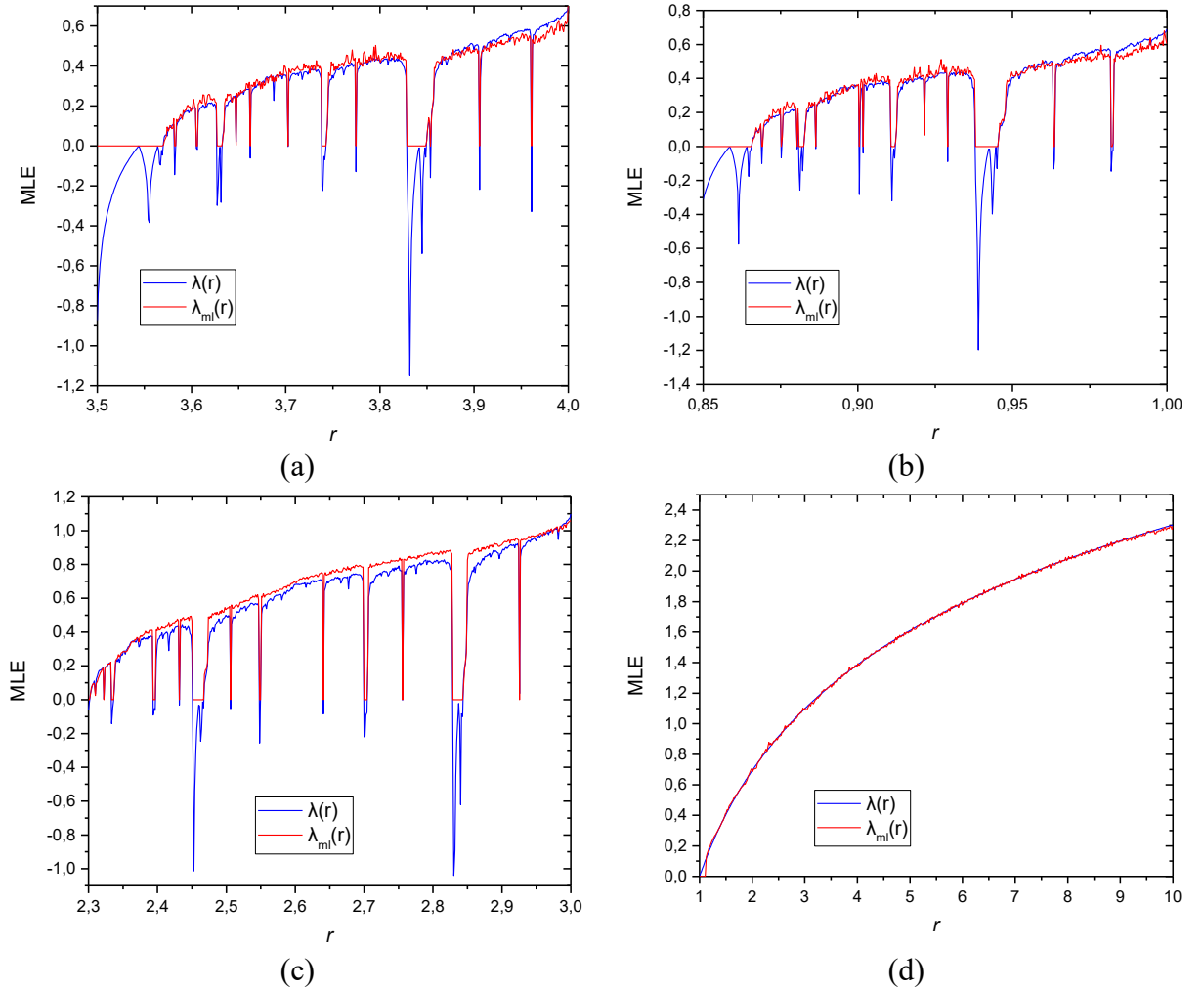
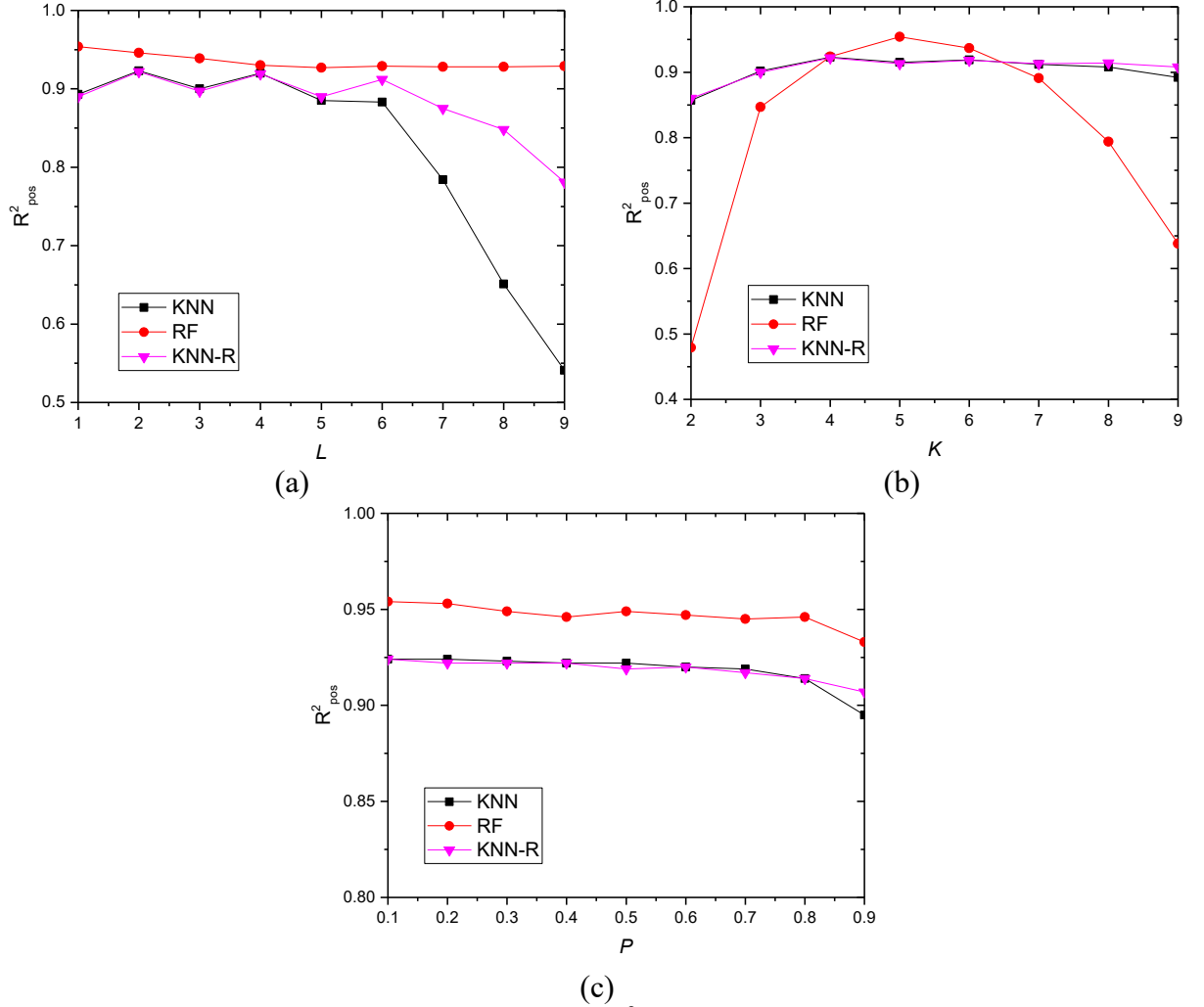


Figure 1. Dependencies  $\lambda_{\text{ml}}(r)$  with minimal errors compared to the reference  $\lambda(r)$  for (a) Logistic Map (RF), (b) Sine Map (RF), (c) Cubic Map (KNN), (d) Chebyshev Map (KNN).

In plots (a)-(c), positive MLE values demonstrate both overestimation and underestimation of  $\lambda_{\text{ml}}(r)$  relative to  $\lambda(r)$  at various points along the curves. For negative MLE values,  $\lambda_{\text{ml}}(r)$  approaches approximately zero.

### 3.2 Influence of Parameters on Estimation Accuracy

To determine the optimal parameter values for calculating the Maximum Lyapunov Exponent (MLE) (see Section 2.3), we analyzed how the accuracy metric  $R^2_{\text{pos}}$  depends on the parameters  $K$ ,  $L$ , and  $P$  for different machine learning models. Figure 2 illustrates the corresponding dependencies of  $R^2_{\text{pos}}$  for the logistic map.



**Figure 2.** Dependencies of prediction accuracy ( $R^2_{\text{pos}}$ ) on segment length ( $L$ ), number of points for slope estimation ( $K$ ), and test subset ratio ( $P$ ), illustrated for different machine learning algorithms (KNN, RF, KNN-R) on the logistic map.

At smaller values of  $L$  (ranging from 1 to 5), the accuracy  $R^2_{\text{pos}}$  exhibits weak dependency on  $L$ . Within this range, changes in  $L$  lead only to minor fluctuations — either slight increases or decreases in accuracy. However, with further increases in segment length ( $L > 5$ ), algorithms such as KNN and KNN-R demonstrate a pronounced reduction in estimation accuracy. Additional series elements, which diverge significantly and thus lack useful predictive information, contribute to decreased prediction accuracy. This deterioration, in turn, can lead to incorrect estimation of the MLE.

In contrast, the Random Forest (RF) model, due to its inherent feature-selection capability when constructing decision trees, minimizes the negative influence of irrelevant elements. As a result, the  $R^2_{\text{pos}}$  curve for RF only marginally decreases for  $L > 5$ , maintaining consistently higher accuracy compared to KNN-based approaches.



The strongest dependence on  $L$  is observed in the KNN algorithm since it utilizes all subset elements equally when computing distances between data points, without differentiating their relevance. In comparison, the KNN-R model — enhanced by a reservoir and principal component analysis (PCA) — shows a reduced sensitivity to increases in  $L < 5$ , as irrelevant information is partially filtered out.

It should also be noted that when analyzing less chaotic time series, increasing  $L$  might actually improve the accuracy of MLE estimation. However, for practical applications involving one-dimensional chaotic maps, selecting a minimal segment length  $L = 1$  is sufficient and typically optimal.

Figure 2b illustrates the dependency of the prediction accuracy metric  $R^2_{\text{pos}}$  on the number of points  $K$ , used to approximate the slope of the line  $\ln(\text{MAE}(N))$  in our proposed method. A distinct optimal region can be observed for all the considered machine learning models.

Initially, as the number of points  $K$  increases, the value of  $R^2_{\text{pos}}$  rises, reflecting a more accurate estimation of the slope of the  $\ln(\text{MAE})$  curve as a function of the prediction horizon  $N$ . However, further increments in  $K$  eventually lead to a decrease in accuracy. This phenomenon arises because, at higher values of the prediction horizon  $N$ , the  $\text{MAE}(N)$  exceeds the standard deviation of the data itself, approaching a constant level regardless of further increases in  $N$ . Consequently, the slope of the line  $\ln(\text{MAE})$  becomes artificially flattened when  $K$  surpasses its optimal value, resulting in reduced accuracy.

Based on the experimental results, optimal values of  $K$  range from 2 to 6 points. Among the tested algorithms, KNN and KNN-R models exhibit the weakest dependence on this parameter, showing greater robustness to changes in  $K$ . Moreover, for time series with smaller MLE values, increasing  $K$  beyond the established optimal range may further improve the estimation accuracy.

The dependency of the prediction accuracy metric  $R^2_{\text{pos}}$  on the proportion  $P$  (ratio of the test subset size to the entire dataset) is represented by a gradually declining curve (see Fig. 2c). For all tested algorithms, accuracy remains relatively stable within the range  $0.1 \leq P \leq 0.8$ , indicating robustness against moderate changes in the training-test split ratio. Only at  $P = 0.9$ , when the size of the training subset becomes significantly smaller, does the accuracy  $R^2_{\text{pos}}$  begin to noticeably decrease. This reduction in performance is attributed to insufficient data available for training at high test-set proportions.

### 3.3 Influence of Time Series Length on Estimation Accuracy

An important characteristic of the proposed MLE estimation method is the minimal required time series length for which the MLE can still be estimated with sufficient accuracy. To investigate this, we constructed the  $R^2_{\text{pos}}(M)$  curves for the KNN, RF, and KNN-R algorithms using the logistic map as a test case. For each series length  $MMM$ , the parameters were individually optimized to achieve the highest possible  $R^2_{\text{pos}}$ .

It is important to note that the reference curves  $\lambda(r)$  were calculated using a series length of  $M = 10,000$ . The results are presented in Figure 3.

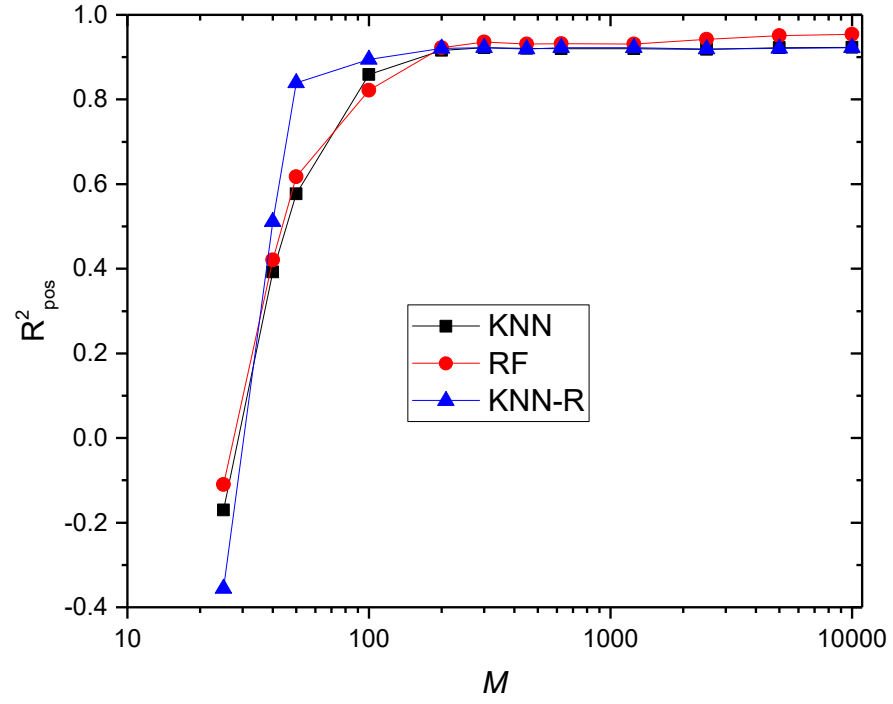


**Figure 3.** Dependence of  $R^2_{\text{pos}}$  on time series length  $M$  for different machine learning algorithms (KNN, RF, KNN-R) using the logistic map.

The findings indicate that for time series longer than  $M = 200$  elements, the estimation accuracy exceeds  $R^2_{\text{pos}} > 0.9$  and is only slightly (less than 5%) lower than the accuracy achieved with a time series of length 10,000. The most significant drop in estimation accuracy occurs when  $M < 200$ .

Among the tested models, the reservoir-based KNN-R algorithm demonstrated the best performance for shorter series: even with  $M = 50$  elements, it achieved an accuracy of  $R^2_{\text{pos}} = 0.839$ , compared to  $R^2_{\text{pos}} = 0.617$  for RF and  $R^2_{\text{pos}} = 0.577$  for KNN. For time series shorter than 25 elements, the estimation accuracy was unsatisfactory for all methods, with  $R^2_{\text{pos}} < 0$ .

### 3.4 Comparative analysis of calculation time

To compare the computational cost of the proposed method across different machine learning models, we conducted a performance benchmark using a time series of length  $M = 10,000$ . For a more reliable estimation, each calculation was repeated 100 times, and the average computation  $t_{\text{comp}}$  was recorded.

The measurements were performed using the following parameters:  $L = 2$ ,  $K = 4$ , and  $P = 0.2$ . The results are summarized in Table 2.

**Table 2.** Average computation time per time series of length  $M = 10,000$  for different machine learning algorithms.

Machine Learning Algorithm	Average Computation Time $t_{\text{comp}}$ , ms
KNN	96
RF	233
MLP	2440
KNN-R	374

The fastest algorithm was KNN. The RF and KNN-R methods were approximately 2 to 4 times slower. The slowest was the MLP model, with a computation time over 25 times greater than that of KNN.

#### 4. Conclusion

This study introduces and systematically validates a novel approach for estimating the maximum Lyapunov exponent (MLE) of chaotic systems using machine learning (ML) models. Unlike traditional machine learning approaches that attempt to directly approximate Lyapunov exponents from time series data, our method leverages the dynamical principle of error growth: the MLE is inferred from the linear increase in the logarithm of the mean absolute prediction error (MAE) as a function of the prediction horizon. To our knowledge, this is the first comprehensive demonstration of applying a general machine learning regression framework — based on out-of-sample trajectory prediction errors — to estimate the Lyapunov exponent for one-dimensional chaotic maps with a single positive exponent.

Our results demonstrate that the proposed approach reliably estimates the positive Lyapunov exponent, with high correspondence ( $R^2_{\text{pos}} > 0.9$ ) to theoretical values across several canonical discrete maps (logistic, sine, cubic, Chebyshev). The method shows robust performance for various ML models (KNN, RF, KNN-R), and the highest accuracy is observed for the Chebyshev and cubic maps. Importantly, we found that the method is effective even for moderate time series lengths ( $M > 200$ ), making it practical for empirical applications where data availability is limited. Reservoir-based models (KNN-R) provided the best accuracy for short time series, highlighting their suitability for experimental scenarios.

A crucial advantage of the proposed technique is its applicability beyond synthetic datasets. Since the method is fundamentally data-driven and relies only on the input-output mapping learned by the ML algorithm, it can be readily extended to real-world time series — including experimental measurements from physical, biological, financial, and engineering systems — where analytical expressions for Lyapunov exponents are unavailable. The only requirement is that the system should possess stationary chaotic dynamics with a positive Lyapunov exponent; extension to multidimensional or nonstationary systems is a promising direction for future research.

Some limitations emerged in our analysis. First, the method is intrinsically limited to estimating positive Lyapunov exponents, as prediction error for stable or periodic regimes does not grow exponentially. Additionally, for very short time series ( $M < 50$ ), estimation accuracy declines for all ML models; longer data is required for reliable estimation. The approach's sensitivity to hyperparameter selection (e.g., segment length  $L$ , number of prediction steps  $K$ , test ratio  $P$ ) and to the choice of ML model underscores the importance of automated model selection and cross-validation for practical deployment.

Several extensions are envisaged. Generalizing the approach to higher-dimensional systems or to systems with multiple positive exponents may require adaptation, such as vector-valued regression or the use of multivariate error metrics. Additionally, integrating domain-specific feature engineering, regularization, and ensemble learning could further improve robustness, especially for noisy or limited data scenarios. Finally, adapting the methodology to nonstationary or transient dynamics — possibly through adaptive windowing or recurrent models — would enhance its applicability to a wider range of real-world problems.

## Acknowledgments

Special thanks to the editors of the journal and to the anonymous reviewers for their constructive criticism and improvement suggestions.

This research was supported by the Russian Science Foundation (grant no. 22-11-00055-P, <https://rscf.ru/en/project/22-11-00055/>, accessed on 10 June 2025).

## Author Contributions

Conceptualization, A.V.; Methodology, A.V., M.B.; Software, A.V. and M.B.; Validation, A.V. and P.B.; Formal analysis, P.B.; Investigation, A.V. and M.B.; Resources, A.V.; Data curation, A.V.; Writing — original draft preparation, A.V., M.B. and P.B.; Writing — review and editing, A.V., M.B. and P.B.; Visualization, M.B.; Supervision, A.V.; Project administration, A.V.; Funding acquisition, A.V. All authors have read and agreed to the published version of the manuscript.

## Conflicts of Interest

The authors declare no conflicts of interest.

## Data availability statement

The data that support the findings of this study are available from the corresponding author, upon reasonable request.

## References

- <sup>1</sup> A. Scott, “Encyclopedia of nonlinear science,” (2006).
- <sup>2</sup> R. Grillo, B.A.Q. Reis, B.C. Lima, L.A.P.F. Pinto, J.B.C. Meira, and F. Melhem-Elias, “The butterfly effect in oral and maxillofacial surgery: Understanding and applying chaos theory and complex systems principles,” *J Craniomaxillofac Surg*, (2024).
- <sup>3</sup> I. Goldhirsch, P. Sulem, and S. Orszag, “Stability and Lyapunov stability of dynamical systems: A differential approach and a numerical method,” *Physica D* **27**, 311–337 (1987).
- <sup>4</sup> K. Li, Q. Wang, C. Hu, B. Liang, C. Jian, Q. Zheng, Z. Tian, and J. Zhao, “Dynamical analysis of a novel 2D Lyapunov exponent controllable memristive chaotic map,” *Chaos: An Interdisciplinary Journal of Nonlinear Science* **34**(8), 083135 (2024).
- <sup>5</sup> J.D. Hart, “Attractor reconstruction with reservoir computers: The effect of the reservoir’s conditional Lyapunov exponents on faithful attractor reconstruction,” *Chaos: An Interdisciplinary Journal of Nonlinear Science* **34**(4), 043123 (2024).
- <sup>6</sup> D. Ayers, J. Lau, J. Amezcua, A. Carrassi, and V. Ojha, “Supervised machine learning to estimate instabilities in chaotic systems: Estimation of local Lyapunov exponents,” *Quarterly Journal of the Royal Meteorological Society* **149**, 1236–1262 (2022).
- <sup>7</sup> D. Wadduwage, C. Wu, and U. Annakkage, “Power system transient stability analysis via the concept of Lyapunov exponents,” *Electric Power Systems Research* **104**, 183–192 (2013).
- <sup>8</sup> E. Aurell, G. Boffetta, A. Crisanti, G. Paladin, and A. Vulpiani, “Predictability in the large: an extension of the concept of Lyapunov exponent,” *Journal of Physics A* **30**, 1–26 (1996).

- <sup>9</sup> G. Cassoni, A. Zaroni, A. Tamer, and P. Masarati, “Stability Analysis of Nonlinear Rotating Systems Using Lyapunov Characteristic Exponents Estimated From Multibody Dynamics,” *J Comput Nonlinear Dyn*, (2023).
- <sup>10</sup> P. Masarati, and A. Tamer, “Sensitivity of trajectory stability estimated by Lyapunov characteristic exponents,” *Aerosp Sci Technol* **47**, 501–510 (2015).
- <sup>11</sup> Q. Zong, W. Yao, H. Zhou, H. Zhao, J. Wen, and S. Cheng, “Transient Stability Assessment of Large-Scale Power System Using Predictive Maximal Lyapunov Exponent Approach,” *IEEE Transactions on Power Systems* **39**, 5163–5176 (2024).
- <sup>12</sup> A. Wolf, J. Swift, H. Swinney, and J. Vastano, “Determining Lyapunov exponents from a time series,” *Physica D* **16**, 285–317 (1985).
- <sup>13</sup> H. Koçak, and K. Palmer, “Lyapunov Exponents and Sensitive Dependence,” *J Dyn Differ Equ* **22**, 381–398 (2010).
- <sup>14</sup> C. Mendes, R. Silva, and M. Beims, “Decay of the distance autocorrelation and Lyapunov exponents,” *Phys Rev E* **99** 6–1, 62206 (2019).
- <sup>15</sup> A. García-García, J. Verbaarschot, and J.-P. Zheng, “Lyapunov exponent as a signature of dissipative many-body quantum chaos,” *Physical Review D*, (2024).
- <sup>16</sup> Y. Lin, “Multi-point Lyapunov exponents of the Stochastic Heat Equation,” *Electron J Probab*, (2023).
- <sup>17</sup> E. Mendes, and E. Nepomuceno, “A Very Simple Method to Calculate the (Positive) Largest Lyapunov Exponent Using Interval Extensions,” *Int. J. Bifurc. Chaos* **26**, 1650226 (2016).
- <sup>18</sup> M. Pollicott, “Maximal Lyapunov exponents for random matrix products,” *Invent Math* **181**, 209–226 (2010).
- <sup>19</sup> B. Eckhardt, and D. Yao, “Local Lyapunov exponents in chaotic systems,” *Physica D* **65**, 100–108 (1993).
- <sup>20</sup> D. McCaffrey, S. Ellner, R. Gallant, and D.W. Nychka, “Estimating the Lyapunov Exponent of a Chaotic System with Nonparametric Regression,” *J Am Stat Assoc* **87**, 682–695 (1992).
- <sup>21</sup> S. Zhou, X.-Y. Wang, Z. Wang, and C. Zhang, “A novel method based on the pseudo-orbits to calculate the largest Lyapunov exponent from chaotic equations,” *Chaos* **29** 3, 33125 (2019).
- <sup>22</sup> J. He, S. Yu, and J. Cai, “Numerical Analysis and Improved Algorithms for Lyapunov-Exponent Calculation of Discrete-Time Chaotic Systems,” *Int. J. Bifurc. Chaos* **26**, 1650219 (2016).
- <sup>23</sup> M. Rosenstein, J. Collins, and C. Luca, “A practical method for calculating largest Lyapunov exponents from small data sets,” *Physica D* **65**, 117–134 (1993).
- <sup>24</sup> Habib, and Ryne, “Symplectic calculation of Lyapunov exponents,” *Phys Rev Lett*, (1995).
- <sup>25</sup> J. Pathak, Z. Lu, B. Hunt, M. Girvan, and E. Ott, “Using machine learning to replicate chaotic attractors and calculate Lyapunov exponents from data,” *Chaos* **27** 12, 121102 (2017).
- <sup>26</sup> C. Mayora-Cebollero, A. Mayora-Cebollero, Á. Lozano, and R. Barrio, “Full Lyapunov exponents spectrum with Deep Learning from single-variable time series,” *Physica D*, (2024).

- <sup>27</sup> J. Pathak, Z. Lu, B.R. Hunt, M. Girvan, and E. Ott, "Using machine learning to replicate chaotic attractors and calculate Lyapunov exponents from data," *Chaos: An Interdisciplinary Journal of Nonlinear Science* **27**(12), 121102 (2017).
- <sup>28</sup> A. Velichko, M. Belyaev, Y. Izotov, M. Murugappan, and H. Heidari, "Neural Network Entropy (NNetEn): Entropy-Based EEG Signal and Chaotic Time Series Classification, Python Package for NNetEn Calculation," *Algorithms* **16**(5), 255 (2023).
- <sup>29</sup> A. Velichko, "A method for medical data analysis using the lognnet for clinical decision support systems and edge computing in healthcare," *Sensors* **21**(18), (2021).
- <sup>30</sup> P. Gaspard, and G. Nicolis, "Transport properties, Lyapunov exponents, and entropy per unit time.," *Phys Rev Lett* **65** **14**, 1693–1696 (1990).
- <sup>31</sup> S.H. Strogatz, "NONLINEAR DYNAMICS AND CHAOS: With Applications to Physics, Biology, Chemistry, and Engineering," *Nonlinear Dynamics and Chaos: With Applications to Physics, Biology, Chemistry, and Engineering*, 1–513 (2018).
- <sup>32</sup> M. Koopialipoor, P. Asteris, A.S. Mohammed, D. Alexakis, A. Mamou, and J. Armaghani, "Introducing stacking machine learning approaches for the prediction of rock deformation," *Transportation Geotechnics*, (2022).
- <sup>33</sup> N. Appiah-Badu, Y. Missah, L. Amekudzi, N. Ussiph, T. Frimpong, and E. Ahene, "Rainfall Prediction Using Machine Learning Algorithms for the Various Ecological Zones of Ghana," *IEEE Access* **10**, 5069–5082 (2022).
- <sup>34</sup> Y.-C. Bo, P. Wang, and X. Zhang, "An asynchronously deep reservoir computing for predicting chaotic time series," *Appl. Soft Comput.* **95**, 106530 (2020).
- <sup>35</sup> J. Viehweg, P. Teutsch, and P. Mäder, "A systematic study of Echo State Networks topologies for chaotic time series prediction," *Neurocomputing* **618**, 129032 (2025).
- <sup>36</sup> M.T. Huyut, A. Velichko, M. Belyaev, Ş. Karaoğlu, B. Sertogullarindan, and A.Y. Demir, "Detection of Right Ventricular Dysfunction Using LogNNet Neural Network Model Based on Pulmonary Embolism Data Set," *Eastern Journal Of Medicine* **29**(1), 118–128 (2024).
- <sup>37</sup> H. Gao, X. Ding, S. Zhang, J. Yu, X. Zhu, Y.-H. Wang, and H. Yang, "KNN-based classification on Alzheimer's disease data after dimensionality reduction using principal component analysis," **12320**, 1232020 (2022).